

# Thin film deposition of transparent materials by rear-side laser ablation: a novel configuration

L. Escobar-Alarcón<sup>1</sup>, M. Villagrán<sup>2</sup>, E. Haro-Poniatowski<sup>3</sup>, J.C. Alonso<sup>4</sup>, M. Fernández-Guasti<sup>3</sup>, E. Camps<sup>1</sup>

<sup>1</sup>Departamento de Física, Instituto Nacional de Investigaciones Nucleares, Apdo. Postal 18-1027, México DF 11801, México (E-mail: lea@nuclear.inin.mx)

<sup>2</sup>Centro de Instrumentos, Universidad Nacional Autónoma de México (E-mail: mayo@aleph.cinstrum.unam.mx)

<sup>3</sup>Departamento de Física, Universidad Autónoma Metropolitana Iztapalapa, Apdo. Postal 55-534, México DF 09340, México (E-mail: haro@xanum.uam.mx)

<sup>4</sup>Instituto de Investigaciones en Materiales, Universidad Nacional Autónoma de México, Apdo. Postal 364, México DF 01000, México (E-mail: alonso@servidor.unam.mx)

Received: 21 July 1999/Accepted: 15 September 1999/Published online: 28 December 1999

**Abstract.** A novel configuration for thin film deposition by rear-side laser ablation is presented. With transparent target materials it is possible to get both front and rear surface laser ablation. In the present work SiO<sub>2</sub> thin films were deposited by rear laser ablation. In order to identify the species in each laser plume the generated plasmas (front and rear) were studied by Optical Emission Spectroscopy. Rear plasma has less ionized species as opposed to the front generated plasma. The deposited films were characterized by IR spectroscopy, ellipsometry and scanning electron microscopy. The results show better stoichiometry but lower evaporation rates for rear-side ablation than those deposited by front-side laser ablation. A simple interference model with a partially coherent source is used to account for the laser ablation process.

**PACS:** 81.15.Fg; 52.75.Rx; 68.55.Jk

Rear-side laser ablation has been investigated using UV and IR laser irradiation in dielectric materials [1–3]. With IR laser irradiation the mechanisms of front and rear-side laser ablation are distinct [1]. In UV-irradiated MgO the differences between front and rear-side ablation mechanisms are more subtle [2]. However, these studies are concerned with the ablation processes only, no reports on the deposition of thin films using rear-side ablation are given. Concerning the theoretical models dealing with laser ablation different possibilities have been investigated; in wide bandgap materials impurity and absorption are supposed to play an important role [4–6]. Furthermore in the case of calcium carbonate at 1.064 μm thermal effects have been computed and found to be negligible [5]. In the present work the preparation and characterization of SiO<sub>2</sub> thin films deposited using rear and front-side laser ablation is presented. A detailed comparison between the films prepared by both methods is made. Furthermore, optical spectroscopy investigations of the corresponding plasmas are presented. The results are discussed

in the frame of a simple interference model proposed to describe front and rear-side laser ablation.

## 1 Experimental setup

There are a number of alternatives to generate the rear plasma, for example, by self-focusing of non-linear materials or in a thick target by focusing the laser at the rear-side. For thin targets two different ways are possible, either by changing the energy per pulse or increasing the optical absorption of the back-side of the target by roughening. In the present work to grow SiO<sub>2</sub> thin films by rear-side laser ablation, we have used this last procedure for the thin (2 mm) SiO<sub>2</sub> targets. The roughening process was performed mechanically by polishing the sample with a coarse grain, and resulted in an enhancement of the exfoliation during the rear side ablation of the sample. Thin films were deposited under vacuum,  $5 \times 10^{-6}$  Torr, using the fundamental frequency of a Nd:YAG laser ( $\lambda = 1064$  nm, pulse duration = 28 ns). The energy per pulse was 280 mJ at a repetition rate of 20 Hz.

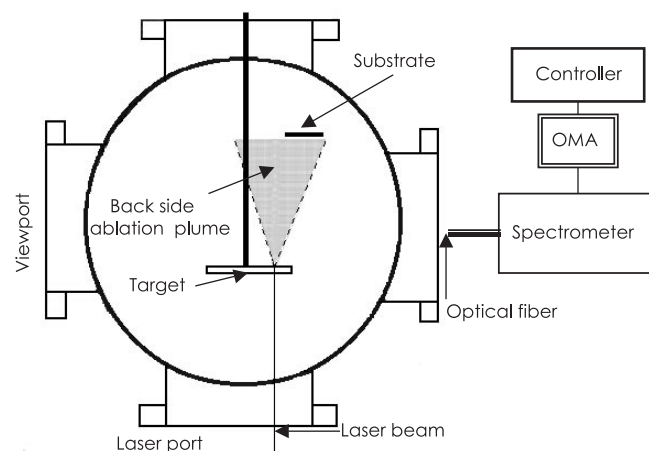


**Fig. 1.** Experimental setup used for deposition of thin films by rear-side laser ablation

The distance between the target and the substrate was kept at about 55 mm. The substrates used were silicon (100) wafers. A schematic diagram of the experimental setup is presented in Fig. 1.

## 2 Infrared spectroscopy

Figures 2a and 2b show the IR transmittance for both SiO<sub>2</sub> films deposited by front (conventional) and rear-side laser ablation. Both spectra show the three major absorption bands corresponding to stretching, bending and rocking motions of the O atoms in the Si–O–Si bridges, which for thermally grown silicon dioxide are located at 1075 cm<sup>-1</sup>, 800 cm<sup>-1</sup> and 450 cm<sup>-1</sup>, respectively [7,8]. In the case of these ablated oxides the main peak (stretching mode) is located at 1033.5 cm<sup>-1</sup> and 1059.32 cm<sup>-1</sup> for SiO<sub>2</sub> films deposited by front and rear-side laser ablation, respectively. It is well known that the shift of this main peak towards lower wavenumbers indicates that these oxides are silicon rich, i.e. SiO<sub>x</sub> with  $x < 2$  [9]. These results are consistent with the ellipsometric measurements since the refractive index of the front ablated oxide is higher than that of

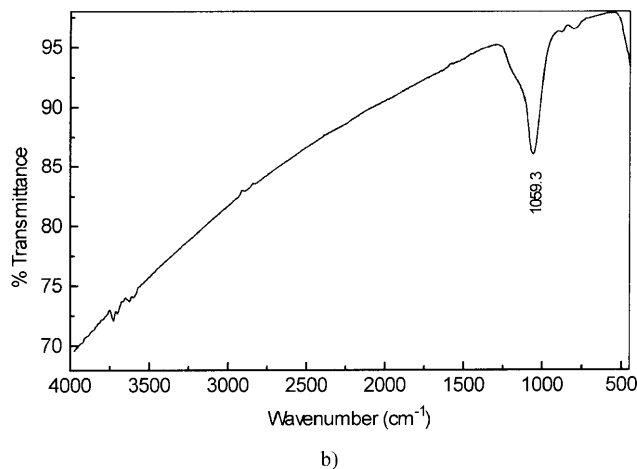
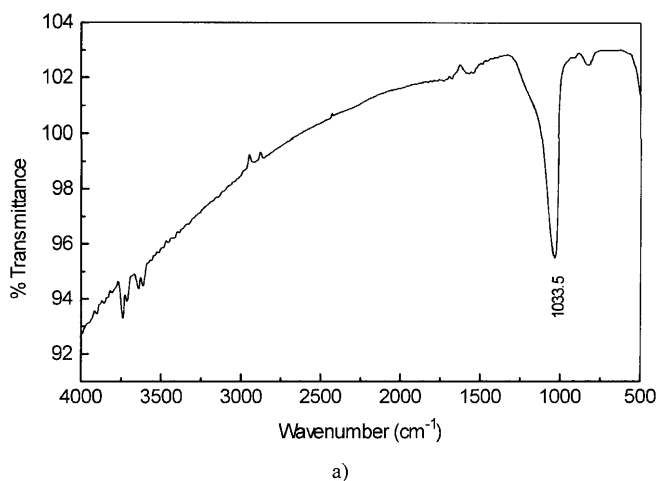


**Fig. 2.** **a** Infrared spectra of the deposited thin films by front-side laser ablation and **b** rear-side laser ablation

the rear ablated oxide whose value is 1.519 and is even higher than that for thermal oxide (1.46). Additionally, two bands related to hydrogen containing bonds such as Si–OH (3380–3620 cm<sup>-1</sup>) or Si–H (930–945 cm<sup>-1</sup>) [10,11] and a band in the region 1600–1630 cm<sup>-1</sup> associated to water [11] are clearly observed in both IR spectra. Since water or hydrogen is absent during the ablation process these results indicate that both oxides are porous and under exposure to the ambient moisture adsorb water. However, the absorption peaks related with hydrogen bonds appear diminished for oxides deposited by rear-side laser ablation. This seems to indicate that oxides deposited by rear laser ablation are less porous than those deposited by front-side laser ablation.

Concerning the surface morphology of the obtained films in both configurations, we have observed that in rear-side laser ablation the films exhibit a greater quantity of splashed particles as compared to the ones grown by frontal laser ablation. This is probably due to the nature of the ablation processes at the front and back surfaces as will be proposed in the model described below.

## 3 Optical emission spectroscopy

We studied the optical emission of both plasmas (front and rear) with an Optical Multichannel Analyzer. The light was collected by a UV-VIS fiber bundle placed at the side window of the chamber, 20 cm apart from the plasma. The exposure time was 0.5 s, working at 20 Hz repetition rate of the laser; ten shots were recorded and integrated. Comparing the spectra of both plasmas from 280 to 500 nm it is observed that the rear plasma has less ionized species, whereas the front plasma is rich in O II (391.2, 413.3 nm) and Si II (333.9, 413.1 nm) ionized species as previously observed by Wolf [12] in a time resolved spectral analysis. In the front plasma the Si II line (290.4 nm) appears clearly while in the rear plasma this line is not observed. Figure 3 shows two spectra, in the front plasma the Si II line (290.4 nm) is observed and in both plasmas the Si I (288.2 nm) is present however in the latter case its intensity is small.

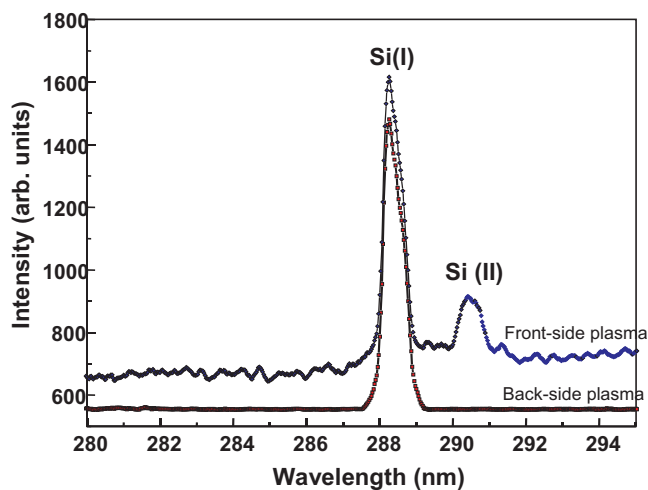


**Fig. 3.** Optical emission spectra of front (*top*) and rear plasmas (*bottom*)

#### 4 Front and back ablation model

Laser ablation has been detected in the front and back surface of transparent targets in several systems [1–3]. It is observed that at moderate powers ablation takes place at the back surface whereas as the power is increased the ablation decreases at the back surface and increases at the front surface until it is only observed at the front surface. Micro photographs also reveal that the ablation at the back surface tends to remove large layers of the bulk material [5]. The damaged area in the back ablation region resembles the slices that are observed in mica and similar stratified materials.

It has been previously proposed that the phase change in the front and back surfaces may account for different effective laser intensities [2]. However, as Yavas et al. [1] point out, the rear and front-side ablation seem to occur by quite different mechanisms. Thermal effects arising from linear absorption have been shown to be negligible in most ablation processes. Defect centers at the surfaces and the diffraction arising from them have also been suggested as relevant mechanisms to explain rear and front ablation [3].

A model that may possibly account for the experimental observations is the interference that takes place between the incident laser beam and the beam reflected from the back surface of the material. The partial coherence of the involved waves plays an important role in the explanation of the various observations. Consider a plane wave propagating at normal incidence into the transparent target with a coherence length  $l_c$ . There is an initial reflection at the front surface of the target, which generates a reflected wave in the semi-space located before the target. The wave intensity just inside the front surface is equal to the transmitted wave intensity rather than the incident plus reflected wave intensities as suggested by Ihlemann [2], since the latter do not penetrate into the material. For this reason, this first reflection is ignored and all that needs to be taken into account is the energy loss due to reflection at the interface. Absorption within the material is considered to be negligible below the ablation threshold and very high above it. Consequently, the wave transmitted from the first surface is equal to the wave incident on the second surface. Upon incidence on the rear surface of the target there is a second reflection which generates a standing wave within the material.

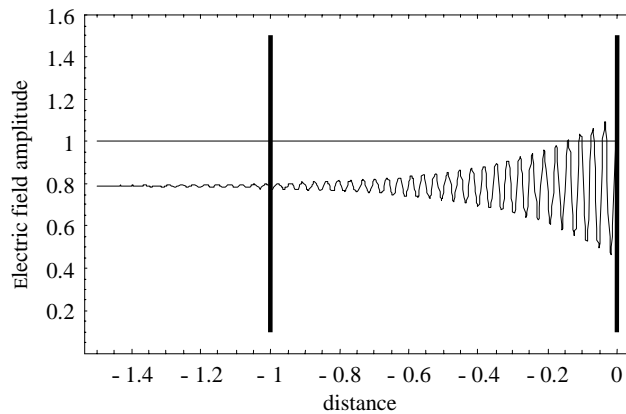


**Fig. 4.** Electric field amplitude vs. distance (A.U.). The sample front and rear surfaces are located at  $-1$  and  $0$  respectively. The field amplitude threshold has been set to  $1$

The intensity of the interference pattern formed within the material due to the waves  $E_{2i}$  and  $E_{2r}$ , propagating in the  $z$  direction, is then  $I = I_{2i} + I_{2r} + 2\sqrt{I_{2i}I_{2r}}\gamma(z)\cos(2kz)$  where the intensity of the  $n$ th wave is  $I_n = E_n E_n^*$  and the coherence function arising from phase fluctuations in a markovian process is given by [13]  $\gamma(z) = \exp[-z/l_c]$  where the origin of  $z$  is placed at the reflection plane of the second surface. The intensity at the reflection plane thus exhibits a maximum of the interference pattern. Due to loss of correlation between the beams, the visibility of the interference pattern decreases as the distance from the reflection plane increases as shown in Fig. 4. In this figure the case where only rear-side ablation occurs is shown.

The ratio of the incident and the reflected wave amplitudes at the rear surface for normal incidence, from the Fresnel equations, is equal to  $\frac{n-1}{n+1}$ , where  $n = \frac{n_{\text{out}}}{n_{\text{mat}}}$  is the ratio of the refractive index outside the material over the refractive index of the target. The intensity within the material is then:

$$I = I_{2i} \left( 1 + \left( \frac{n-1}{n+1} \right)^2 + 2 \left( \frac{n-1}{n+1} \right) e^{-\frac{z}{l_c}} \cos(2kz) \right)$$

the incoherent intensity  $I_{2\text{inc}}$  is obtained from the above equation in the limit when the exponent tends to zero, whereas the maximum intensity near the reflection plane  $I_{2\text{max}}$  obtained when the coherence function and the cosine term are equal to one.

Let us assume that the coherence length  $l_c$  is shorter than the target optical thickness  $n_{\text{mat}}$ , where  $d$  is the target thickness. The intensity at the front surface may then be approximated to be equal to the incoherent intensity. Whereas at the rear surface there are maximum intensity planes separated by half the wavelength. The ratio of these two intensities is:

$$\begin{aligned} \frac{I_{2\text{max}}}{I_{2\text{inc}}} &= \left( 1 + \left( \frac{n-1}{n+1} \right)^2 \right) / \left( 1 + \left( \frac{n-1}{n+1} \right)^2 \right) \\ &\approx 1 + 2 \left( \frac{n-1}{n+1} \right) \end{aligned}$$

Let  $I_{\text{th}}(\text{front})$  be the threshold ablation intensity for the material. This is the threshold for front-side ablation without any reflection on the back surface of the target. Upon reflection, the threshold in the back surface decreases by a factor given by the quotient established in the above equation. The rear surface ablation threshold is then  $I_{\text{th}}(\text{rear}) \approx I_{\text{th}}(\text{front}) / \left[ 1 + 2 \left( \frac{n-1}{n+1} \right) \right]$ .

When the incident intensity is higher than  $I_{\text{th}}(\text{rear})$  but lower than  $I_{\text{th}}(\text{front})$ ; ablation only takes place near the back surface. The regions where the wave amplitude is above the rear ablation threshold depend on the angle of the incident beam. Consider for simplicity normal incidence. The ablation planes are then slices parallel to the back surface separated by half wavelengths. Apart from the outermost plane, ablation of material within the inner planes will have to thrust away non-ablated material lying in the regions where interference yields a field amplitude below threshold. Slices of material in the bulk will then be ejected in addition to plasma arising from the hotter regions. This process would account for the increased splashing in rear ablation as well as the sliced structure of damage on the target observed by several authors. Furthermore, the plasma generated

in the inner planes will lose some of their energy breaking down the material in front of them and thus lower energy plasmas are expected, which is what we observe in optical emission spectroscopy. Once the incident intensity reaches  $I_{th}(front)$  ablation takes place in the front surface only.

In order to account for ablation in both surfaces simultaneously, it seems necessary to include the intensity profile of the incident beam. That is, to consider for example a Gaussian beam rather than a plane wave. The center part of the beam would then be above  $I_{th}(front)$  and produce front ablation whereas a surrounding ring of the beam is greater than  $I_{th}(rear)$  but lower than  $I_{th}(front)$ ; producing back ablation. At high intensities, most of the beam energy lies above the front threshold and only front ablation is obtained. On the other hand, if the rear-side roughening features become comparable with the excitation wavelength, then a theory including scattering from random rough surfaces must be included [14]. Such a treatment will reveal additional effects such as enhanced back scattering.

*Acknowledgements.* The present work has been partially supported by the Consejo Nacional de Ciencia y Tecnología of México under contract num-

ber: 4225-E9405. The authors appreciate the assistance of Ruben Gomez (ININ) with the Nd:YAG laser used in the present work.

## References

1. O. Yavas, E.L. Maddocks, M.R. Papantonakis, R.F. Haglund, Jr.: Appl. Phys. Lett. **71**, 1287 (1997)
2. J. Ihlemann: Appl. Surf. Sci. **54**, 193 (1992)
3. R.L. Webb, S.C. Langford, J.T. Dickinson: J. Appl. Phys. **80**, 7057 (1996)
4. R.F. Haglund, Jr., R. Kelly: *Fundamental processes in sputtering of atoms and molecules*, ed. by P. Sigmund (The Royal Danish Academy of Sciences and Letters, Copenhagen) p.527 (1993)
5. O. Yavas, E.L. Maddocks, M.R. Papantonakis, R.F. Haglund, Jr.: Appl. Surf. Sci. **127-129**, 26 (1998)
6. T. de Rességuier, F. Cottet: J. Appl. Phys. **77**, 3756 (1995)
7. W.A. Pliskin: J. Vac. Technol. **14**, 1064 (1977)
8. P. Lange: J. Appl. Phys. **66**, 201 (1989)
9. P.G. Pai, S.S. Chao, Y. Takagi, G. Lukovsky: J. Vac. Technol. A **14**, 689 (1986)
10. J.A. Theil, D.V. Tsu, M.W. Watkins, S.S. Kim, G. Lukovsky: J. Vac. Sci. Technol. A **8**, 1374 (1990)
11. G. Socrates: *Infrared characteristics group frequencies tables and charts* (Wiley, New York 1994)
12. P.J. Wolf: J. Appl. Phys. **72**, 1280 (1992)
13. M. Sargent III et al.: *Laser Physics* (Addison Wesley 1974) pp.84-88
14. J.A. Ogilvy: *Theory of wave scattering from random rough surfaces* (Adam Hilger, Bristol 1991)